Iron(III) complexation behavior of benzene-centered tripodal mono-, di- and tritopic ligands carrying a repeating –Ahe–(HO)Apr– sequence [Ahe = 6-aminohexanoyl; (HO)Apr = 3-(*N*-hydroxy)-aminopropanoyl]†

Akira Tsubouchi, Langtao Shen, Yukihiro Hara and Masayasu Akiyama*

Department of Applied Chemistry, Tokyo University of Agriculture and Technology, Koganei, Tokyo 184-8588, Japan. E-mail: akiyama@cc.tuat.ac.jp

Received (in Montpellier, France) 17th July 2000, Accepted 24th October 2000
First published as an Advance Article on the web 4th January 2001

To investigate how three-directional molecules behave upon complexation with ferric iron, tripodal 1,3,5-benzene-centered mono-, di- and tritopic iron-chelating ligands $\{C_6H_3[CO–(Ahe–(HO)Apr)_n–OH]_3$: **1**, $n = 1$; **2**, $n = 2$; **3**, $n = 3\}$, composed of strands containing an –Ahe–(HO)Apr– sequence [Ahe = 6-aminohexanoyl; (HO)Apr = 3-(*N*-hydroxy)aminopropanoyl], were synthesized. These hydroxamate ligands form intramolecular six-coordinate octahedral complexes with Fe(III): Fe_1-**1**, Fe_1-**2**, Fe_2-**2**, Fe_1-**3**, Fe_2-**3** and Fe_3-**3**. The complexes formed were investigated from a topological viewpoint and examined in terms of stability against attack by H^+ and HO^-, monoprotonation equilibrium and iron removal kinetics using a 20-molar excess of EDTA. Fe_1-**1**, Fe_1-**2** and Fe_2-**2** have tripodal interstrand structures. In particular, the iron removal reaction of Fe_2-**2** shows a consecutive first-order reaction pattern. From kinetic data of the first-order reactions, Fe_1-**3**, Fe_2-**3** and Fe_3-**3** are concluded to possess one, two and three discrete ferrioxamine-type (intrastrand) structures, respectively.

Siderophores are low molecular weight, iron-chelating compounds produced by microorganisms to acquire the metal ion from the environment.[1–5] Desferrioxamines (iron-removed ferrioxamines) and desferrichromes (iron-removed ferrichromes) are two representative families of naturally abundant hydroxamate siderophores.[6–8] The three hydroxamate groups in the linear and cyclic oligoamides of the former and those in the three ornithine side chains of cyclohexapeptides of the latter form stable six-coordinate complexes with iron(III).[9–11] The iron complexes of these families present different topologies and are recognized by different kinds of receptors upon microbial iron uptake.[7,12–16]

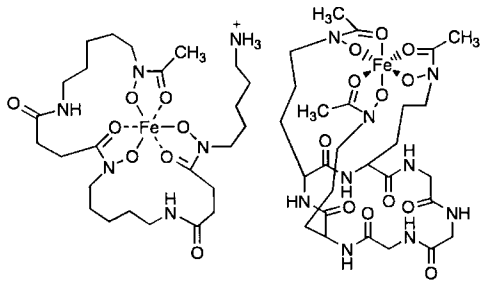

Ferrioxamine B Ferrichrome

In effort to better understand the biological activity of hydroxamate siderophores, a variety of iron-chelating compounds that mimic certain characteristics of natural substances have been designed and synthesized.[17–19] Among them, 1,3,5-trisubstituted benzene-centered monotopic hydroxamate ligands represent one type of tripodal ligand; their iron-coordination and biological activity as well as various chemical properties of the complexes have been studied.[20–24] Previously we reported retro-hydroxamate desferrioxamines E and G, which have the hydroxamate groups transposed relative to their natural counterparts.[25] This synthesis has brought some flexibility to the design and synthesis of hydroxamate iron-binding compounds. In the course of extending these studies, a question occurs: when three linear desferrioxamine-type strands are combined together by a tripodal molecule, how does the resulting three-directional molecule behave upon complexation with three ferric ions, that is, which type of structure is produced, a tripodal interstrand-type structure or a discrete ferrioxamine-type intrastrand structure? Either could provide a potential basis to fabricate functionalized compounds on its extended molecular array.[26] In addition to the topological question, multitopic iron-chelating compounds will exhibit allosteric or cooperative behavior upon iron–ligand exchange reactions or iron–complex formation, as Shanzer's group observed a triple helical structure with their ditopic iron-binders.[27] Furthermore, such iron chelators have potential for the development of clinical iron-removal agents, as the test results with the relatively larger hydroxamate-carrying molecules show.[28,29]

To address these questions, we undertook the synthesis of 1,3,5-benzene-centered tripodal mono-, di- and tritopic iron-chelating compounds composed of a suitable hydroxamate-containing segment. By taking advantage of our previous synthesis,[25] the –Ahe–(HO)Apr– sequence [Ahe = 6-aminohexanoyl; (HO)Apr = 3-(*N*-hydroxy)aminopropanoyl] was used as a synthetic unit, and a series of tripodal hydroxamate ligands that contain strands of up to the three repeated sequences, retro-hydroxamate desferrioxamine G, were synthesized. In di- and tritopic ligands, the hydroxamic acid groups in each strand are separated by a 9-atom spacer. This spacing allows ferric ions to produce less strained complexes either in a tripodal interstrand or a linear intrastrand way. The iron complex formation, the stability of the formed complexes against H^+ attack, and iron removal kinetics from the complexes by EDTA are investigated here by focusing on the topological problem.

† Electronic supplementary information (ESI) available: synthesis and characterization of the intermediate species **6**–**9** and **13**–**18**. See http://www.rsc.org/suppdata/nj/b0/b005788f/

Results

Syntheses

Benzyl (Bn), *tert*-butoxycarbonyl (Boc), and methyl groups were used as the protecting groups, where necessary. The synthetic unit, Boc–Ahe–(BnO)Apr–OMe, was obtained *via* the acylation of H–(BnO)Apr–OMe with Boc–Ahe–OH by the mixed anhydride method using isobutyl chloroformate (IBCF).[30] Protected di- and trihydroxamic acid units, Boc–[Ahe–(BnO)Apr]$_n$–OMe (n = 2, 3), were synthesized by repetitive condensation of H–Ahe–(BnO)Apr–OMe and H–[Ahe–(BnO)Apr]$_2$–OMe with Boc–Ahe–(BnO)Apr–OH using 1-ethyl-3-[3-(dimethylamino)propyl]carbodiimide (EDC) as the condensation reagent.[31] Triethylamine (Et_3N) was used when necessary.

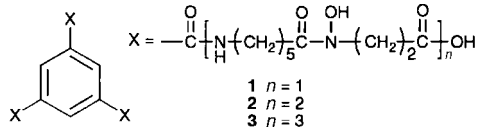

The tripodal ligands (**1**–**3**) were synthesized by condensation of the N-terminal free amine units, H–[Ahe–(BnO)Apr]$_n$–OMe (n = 1, 2, 3), with 1,3,5-benzenetricarbonyl trichloride, and then the methyl ester groups of the resulting benzene-centered tripodal molecules were hydrolyzed, followed by hydrogenation to remove the benzyl groups. The synthesis of the ligands is illustrated in Scheme 1. The purity of **1**–**3** was checked by HPLC, and their structures were characterized by IR, ^{1}H NMR spectroscopy and elemental analysis. Key NMR signals observed were the three benzene-ring protons and the CON(OH)–CH_2– methylene protons (centered at 3.68 ppm); in addition the signal intensity of the latter protons indicated the full presence of the hydroxamic acid groups in ligands **1**–**3**. The ligands possess the chain terminal carboxylic acid groups and are soluble in a slightly alkaline solution, and only sparingly soluble in an aqueous acidic solution.

Iron(III) complex formation

Iron(III) complexes were prepared by adopting a procedure previously described.[32] When an aqueous solution of a ligand was mixed with an acidic ferric nitrate solution, a complex was produced in the solution (*ca.* pH 2.2). The complex at this stage consisted of mainly a di(aquo)bis(hydroxamato)iron(III) species, Fe(HL)$^+$ with a λ_{max} of 465 nm.[33,34] This species was converted into a tris(hydroxamato)iron(III) species (a 1 : 3 complex of a ferric ion with a hydroxamate group), Fe(L), by gradual neutralization with alkali to pH 7. Mono- and dinuclear complexes were prepared with **2**, and mono-, di- and trinuclear complexes were produced with **3**. In the case of **3**, a 15% DMF aqueous ligand solution was used, and the resulting final iron(III) complex solution contained 5% DMF v/v. The complex solutions were used for further investigations after twofold dilution with water. The formation of iron(III) complexes was further confirmed by the ESI mass spectra. These tris(hydroxamato)iron(III) complexes are designated as Fe-**1**, Fe$_1$-**2**, Fe$_2$-**2**, Fe$_1$-**3**, Fe$_2$-**3** and Fe$_3$-**3**, respectively.

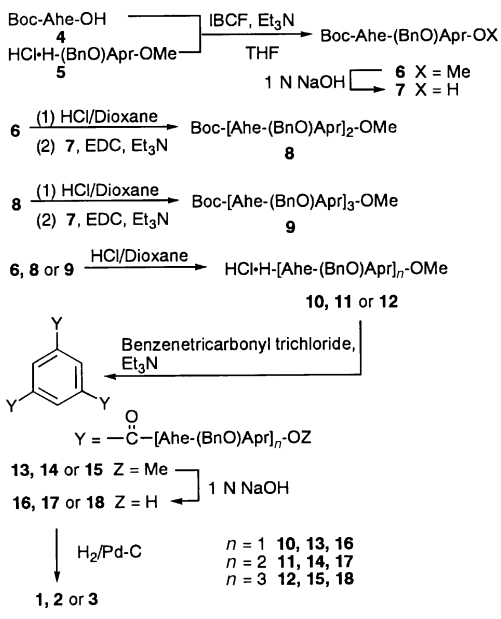

Scheme 1

UV-vis spectroscopy

The UV-vis spectra of the above complexes at neutral pH showed the characteristic absorption at λ_{max} 420 nm with *ca.* ε 3000/Fe M^{-1} cm^{-1}, typical of tris(hydroxamato)iron(III) complexes.[4,33] In determining individual ε values of multitopic iron(III) complexes, plots were made for absorbance at 420 nm against the molar ratio of iron(III) to each ligand (**2** or **3**) at pH 7.0, shown for **3** as an example in Fig. 1. A straight line passing through the origin of both ordinate and abscissa demonstrates an equivalent ε value for each iron at the three binding sites (the same is also true at the two binding sites in **2**, not shown). Ferric ion, added in excess over a 3-equivalent amount, precipitated out of the solution.

Plots of the ε values at 420 nm *vs.* pH show plateau regions, where the iron species exist as a tris(hydroxamato)iron complex (Fig. 2). The spans of these plateaus allows us to estimate the stability of the tris(hydroxamato)iron(III) complexes against attack by H^+ or OH^- ions. The stability increases in the order Fe$_1$-**1** < Fe$_2$-**2** < Fe$_1$-**2** < Fe$_3$-**3** < Fe$_1$-**3** ≈ Fe$_2$-**3**.

When a neutral complex solution was gradually acidified, the λ_{max} shifted to longer wavelength and its ε value decreased.[33] An isosbestic point was observed for individual iron complexes, for example, as shown for Fe$_2$-**2** at 475 nm (Fig. 3). Isosbestic behavior indicates a protonation equilibrium between Fe(L) and Fe(HL)$^+$ [eqn. (1)], confirming the presence of Fe(L).

$$Fe(L) + H^+ \rightleftharpoons Fe(HL)^+ \quad (1a)$$

$$K_{Fe(HL)} = [Fe(HL)^+]/[Fe(L)][H^+] \quad (1b)$$

For Fe$_2$-**2**, shown in Fig. 3, the pH range and the magnitude of its absorbance indicate the formation of Fe(L^{lower})–Fe(HL^{upper}) (*vide infra*), when ligand **2** is expressed as H_3L^{lower}–H_3L^{upper}.

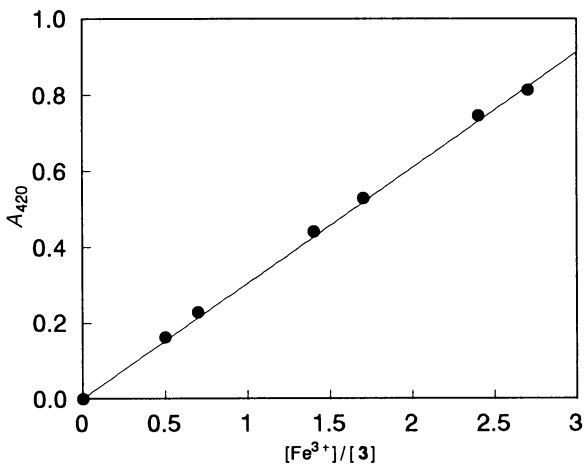

Fig. 1 Plot of absorbance at 420 nm for complexes of **3** *vs.* the molar ratio [Fe^{3+}]/[**3**] at pH 7.0, showing a linear dependence.

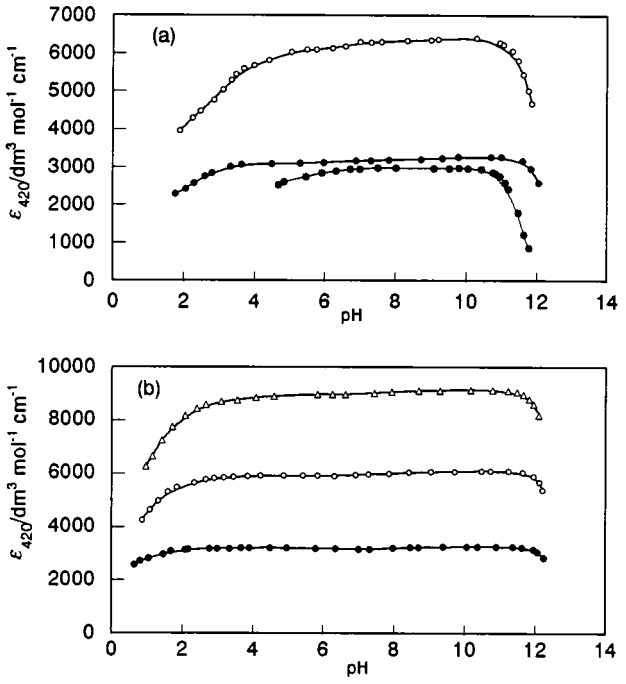

Fig. 2 Values of ε/dm^3 mol^{-1} cm^{-1} at 420 nm in water at 25 °C are plotted against pH (pH meter readings): (*a*) Fe_1-**1** (lower ●), Fe_1-**2** (upper ●) and Fe_2-**2** (○); (*b*) Fe_1-**3** (●), Fe_2-**3** (○) and Fe_3-**3** (△); all the solutions of complexes with **3** contained 2.5% DMF. Readings of pH meter below 2 and above 11 are given for comparison.

The equilibrium was further analyzed by applying the Schwarzenbach equation [eqn. (2)] to the spectral data (absorbance at 420 nm).[33] The resulting plot is shown in the inset of Fig. 3.

$$A_{obs} = (A_0 - A_{obs})/[H^+]K_{Fe(HL)} + \varepsilon_{Fe(HL)}\, c_{total} \quad (2)$$

The $K_{Fe(HL)}$ values (Table 1) indicate the relative ease of monoprotonation of the tris(hydroxamato)iron(III) complexes to form $Fe(HL)^+$. The values for Fe_1-**1**, Fe_1-**2** and Fe_2-**2** show

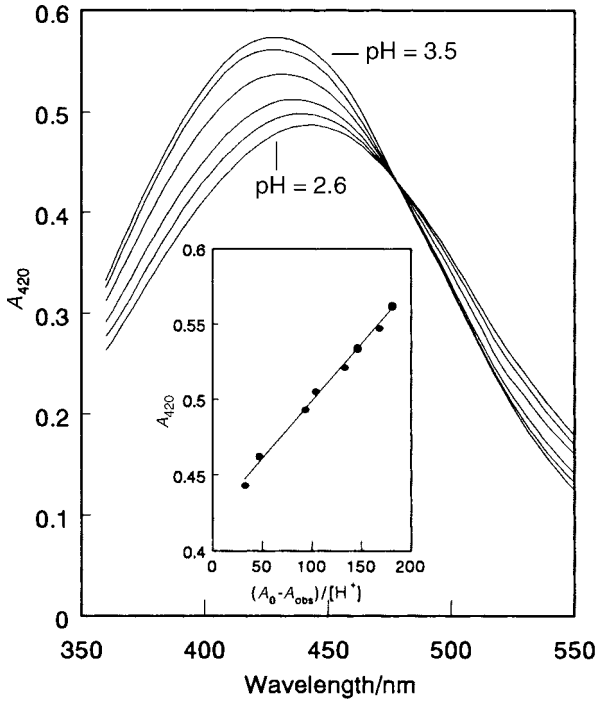

Fig. 3 UV-vis spectra of Fe_2-**2** in the pH range 3.5–2.6 in water at 25 °C, showing an isosbestic point at 474 nm. A Schwarzenbach plot for the same pH range is shown in the inset.

Table 1 UV–vis spectra of tris(hydroxamato)iron(III) complexes and their monoprotonation constants $K_{Fe(HL)}$

Complex	λ_{max}/nm (ε/M^{-1} cm^{-1})[a]	$K_{Fe(HL)}$[b]
Fe_1-**1**	420(2980)	2.3×10^5
Fe_1-**2**	420(3150)	2.3×10^2
Fe_2-**2**	420(6300)	1.3×10^3
Fe_1-**3**	420(3050)	12
Fe_2-**3**	420(6100)	12
Fe_3-**3**	420(9150)	26

[a] Complexes of **1** and **2** were determined in water and those of **3** in an aqueous solution containing 5% DMF at pH 7.0 at 25 °C. [b] Complexes of **3** determined in aqueous 2.5% DMF solution; values of less than 30 are only useful for rough comparison.

great ease of monoprotonation, compared with those for Fe_1-**3**, Fe_2-**3** and Fe_3-**3**.

Iron(III) exchange with EDTA

The iron-binding ability of these tris(hydroxamato)iron(III) complexes was investigated kinetically by exchanging its ligand with a competing ligand, ethylenediaminetetraacetic acid (EDTA).[32,35,36] The proton-assisted iron-removal reaction from Fe(L) with EDTA is described by eqn. (3), as reported for ferrioxamine B,[35] and as supported by our data.[37]

$$Fe(L) + H^+ \rightleftharpoons Fe(HL)^+ \quad (3a)$$

$$Fe(HL)^+ + H_2EDTA^{2-} \rightleftharpoons (HL)Fe(H_2EDTA)^- \rightleftharpoons H_3L + Fe(EDTA)^- \quad (3b)$$

The rate of the iron-removal reaction in the presence of a 20-fold molar excess of EDTA, that is, under conditions for a pseudo-first-order reaction with respect to Fe(L), was determined at pH 5.4 by following the decrease in the absorbance of Fe(L) at 420 nm with time. The removal reactions for the monoferric complexes Fe_1-**1**, Fe_1-**2** and Fe_1-**3** obeyed a first-order rate law, and their rates were determined as pseudo-first-order rate constants. However, in the case of Fe_2-**2** a pseudo-first-order kinetic process was not observed rather its rate behavior appeared to be biphasic. This situation was analyzed by assuming that consecutive first-order rate relations apply,[38] such that the overall removal process is described by the pseudo-first-order rate constants k_1^{up} and k_1^{down} for the removal of the irons from the upper and lower sites. The absorbance (A_t) at time t is thus expressed by eqn. (4) using the initial absorbance (A_0).

$$A_t = A_0 \exp(-k_1^{up}t) + \tfrac{1}{2}A_0[k_1^{up}/(k_1^{up} - k_1^{low})] \times [\exp(-k_1^{low}t) - \exp(-k_1^{up}t)] \quad (4)$$

The progress of the reaction of Fe_2-**2** (absorbance changes *vs.* time) is depicted in Fig. 4; the solid line is a fit of eqn. (4) to the experimental points.

Unlike Fe_2-**2**, the reactions of Fe_2-**3** and Fe_3-**3**, in which multiple iron removal was also involved (*vide infra*), did not show consecutive first-order rate processes. Instead the reactions conformed to a first-order rate law, suggesting the formation of two discrete intrastrand complexes for Fe_2-**3** and three intrastrand ones for Fe_3-**3**. The obtained rates are summarized in Table 2.

Intrastrand *vs.* interstrand complexes

In order to compare the iron-holding capacity of the intrastrand complexes with that of the interstrand complexes, we carried out equilibrium iron-exchange competition reactions [eqn. 5(a)] on an equimolar basis at a constant pH (=5.4), using two tris(hydroxamato)iron(III) complexes, tripodal interstrand Fe_1-**2** and a ferrioxamine-type intrastrand complex

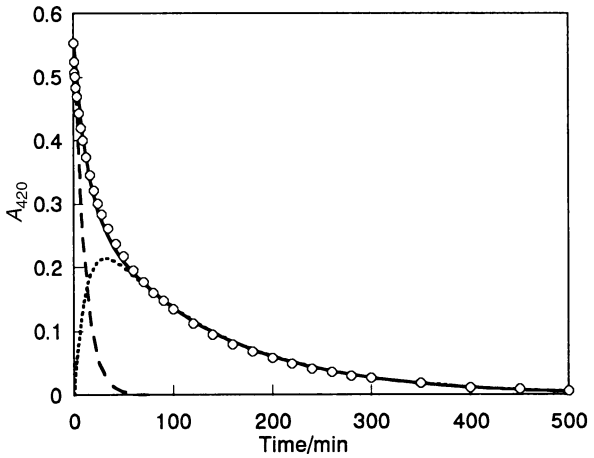

Fig. 4 Absorbance change over time for iron(III) removal from Fe_2-**2** by excess EDTA in water at 25 °C. The observed absorbance changes at 420 nm (○) are plotted, together with a solid curve based on eqn. (4) obtained by varying the constants k_1^{up} and k_1^{low} to provide the best fit to the data points. The dotted and the broken lines show the absorbance contributions from the intermediate state Fe_1-**2** and the remaining Fe_2-**2**, respectively. The absorbance value of the final state $Fe(EDTA)^-$ can be neglected here because it makes only a small contribution. Values of k_1^{up} and k_1^{low} are given in Table 2.

(retro-hydroxamate *N*-acetylferrioxamine G methyl ester, RFG), Fe–{Ac–[Ahe–(O^-)Apr]$_3$–OMe}. The reactions were examined at three temperatures in the range 18.5–35 °C, in order to determine the thermodynamic parameters (ΔG, ΔH, ΔS) of the equilibrium.

Table 2 Rates of iron removal from tris(hydroxamato)iron(III) complexes by EDTA[a]

Complex	Removal rate/s^{-1}
Fe_1-**1**	1.2×10^{-2}
Fe_1-**2**	1.4×10^{-4} (lower site)
Fe_2-**2**	1.6×10^{-3} (upper site)
	1.4×10^{-4} (lower site)
Fe_1-**3**	2.7×10^{-5}
Fe_2-**3**	2.2×10^{-5}
Fe_3-**3**	2.5×10^{-5}
Ferrioxamine B	1.7×10^{-5}

[a] Reaction conditions: [iron complex] = 1.0×10^{-4} M, [EDTA] = 2.0×10^{-3} M; AcOH–AcONa buffer (40 mM) at pH 5.4, temperature 25 °C and ionic strength 0.1 (KNO_3). The rates were determined with errors of ±5% except for Fe_2-**2**. The consecutive first-order rates for Fe_2-**2** were calculated with errors less than ±3%.

Table 3 Iron(III)-exchange equilibrium reactions for Fe_1-**2** and RFG at different temperatures[a]

T/°C	Remaining complex (%)		K_{eq}[b]/M^{-1}
18.5	Fe_1-**2**[c]	34	9.3×10^6
	RFG[c]	49	2.8×10^6
25	Fe_1-**2**	29	1.5×10^7
	RFG	41	5.2×10^6
35	Fe_1-**2**	26	2.1×10^7
	RFG	33	1.0×10^7
Complex	$\Delta H°$/kJ mol^{-1}		$\Delta S°$/kJ mol^{-1} T^{-1}
Fe_1-**2**	36		0.26
RFG	58		0.32

[a] Conditions: [Fe(L)] = [H_2EDTA^{2-}] = 2.5×10^{-4} M; in water at pH 5.4 and ionic strength 0.1 (KNO_3). [b] K_{eq} is defined by eqn. 5(b), (R = 8.315 J mol^{-1} K^{-1}). [c] Fe_1-**2**: Fe–C_6H_3[CO– Ahe–(O^-) Apr–Ahe–(HO)Apr–OH]$_3$; RFG (a retro-ferrioxamine G derivative): Fe–{Ac–[Ahe–(O^-)Apr]$_3$–OMe}.

$$Fe(L) + H_2EDTA^{2-} + H^+ \rightleftharpoons Fe(EDTA)^- + H_3L \quad (5a)$$

$$K_{eq} = [Fe(EDTA)^-][H_3L]/[Fe(L)][H_2EDTA^{2-}][H^+] \quad (5b)$$

$$\Delta G° = \Delta H° - T\Delta S° = -RT \ln K_{eq} \quad (5c)$$

The equilibrium constant K_{eq} of eqn. 5(b) was calculated from the concentrations of Fe(L) and the species involved in the reaction at equilibrium using the mass balance of eqn. 5(a). A van't Hoff plot of ln K_{eq} *vs.* T^{-1} [eqn. 5(c)] for each reaction was linear, yielding ΔH from the slope and ΔS from the intercept. The results are given in Table 3.

In the equilibrium competition reaction between Fe(L) and EDTA, a larger proportion of Fe(L) remained with RFG than with Fe_1-**2**.

Biological activity

Microbial growth promotion tests using an *Escherichia coli* mutant were performed by the published procedure.[12] The test did not show any iron-transport activity for these iron(III) complexes. Similar negative results were reported for analogous benzene-centered tris(hydroxamato)iron(III) complexes.[22]

Discussion

Ligands

By combining the synthetic units, H–[Ahe–(BnO)Apr]$_n$–OMe (n = 1–3), and 1,3,5-benzenetricarboxylic acid and finally removing their protecting groups, good yields of the tripodal mono-, di- and tritopic iron(III) binding ligands (**1**, **2** and **3**) were obtained. All the ligands have chain terminal carboxylic acid groups, which affected their chemical behavior upon iron complexation. Ligands **1** and **2** were soluble in aqueous solution despite the presence of both apolar benzene ring and pentamethylene units, and ligand **3** was soluble in a 15% DMF aqueous solution. The chain length between the 1,3,5-benzene carboxyamido and the first hydroxamate group of **1** is five atoms long, the same as that of our previously tested ligand, 1,3,5-C_6H_3[$CONHCH_2CH_2OCH_2CH_2N(OH)COCH_3$]$_3$, which formed an intramolecular tris(hydroxamato)complex with iron(III).[24]

Types of iron complexes

The iron(III) complexes were prepared by the previous procedure without any difficulty,[32] complexes **1** and **2** were studied in aqueous solution and those of **3** were studied in aqueous 2.5% DMF solution. The DMF content had a negligible effect on pH and it was regarded as a virtually aqueous solution. It is notable that each of the mono- and oligonuclear tris(hydroxamato)iron(III) complexes of ligands **2** and **3** exhibited an equal ε value per Fe. This made the kinetic analysis of multitopic complexes much easier. The confirmation of individual tris(hydroxamato)iron(III) complexes of **1**, **2** and **3** was made by observing their isosbestic points during the pH-dependent transformation between $Fe(HL)^+$ and Fe(L). Isosbestic behavior strongly indicates that the complexes are formed within a single ligand (intramolecular type); if interligand complexes (intermolecular type) were formed by coordination of more than two ligands to one iron(III), no isosbestic point could be observed because of the different constitutions of the resulting complexes. Consequently, the mono- and dinuclear iron complexes with **1** and **2** were concluded to have tripodal intramolecular interstrand structures (Scheme 2.)

In the case of Fe_2-**2**, the tripodal intramolecular interstrand complexation produced a double-layered structure, which was characterized by the iron-removal behavior. The iron-removal reaction in general proceeds *via* intermediate ternary complex

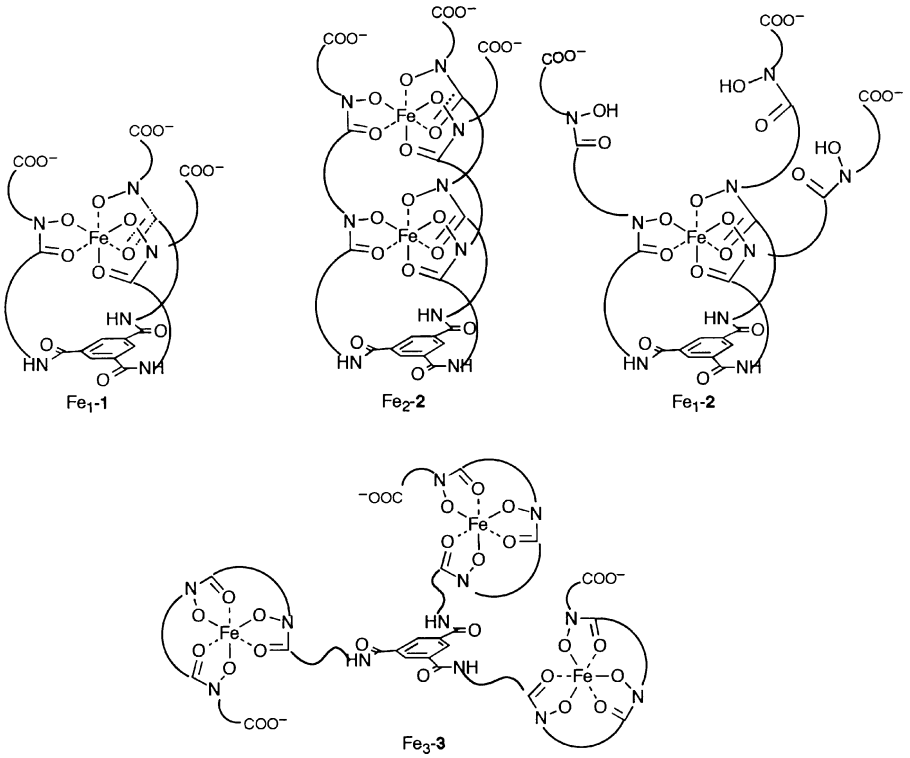

Scheme 2

formation with the competing ligand EDTA;[35,36] therefore, the iron at the lower site is removed only after removal of the iron at the upper site. Consistent with this double-layered complexation, the two irons in Fe_2-**2** were removed with different rates from the upper and lower sites.

For Fe_1-**2**, there was the possibility that the iron can reside at either the lower or the upper sites, but this ambiguity was ruled out by the observation of monophasic rate behavior, corresponding to iron residence at the lower site.

There are two possible iron-binding modes for intramolecular complex formation of ligand **3**; one is a tripodal interstrand mode and the other is a discrete ferrioxamine-type intrastrand one. If the former is the case, iron removal from a multiple-iron loaded ligand, for example with Fe_2-**3**, should be observed as a consecutive iron-removal process, as in the case of Fe_2-**2**. However, iron removal from Fe_2-**3** proceeded at the same rate for its iron, and also Fe_3-**3** showed the same rate for its total iron. These two complexes, therefore, do not have multi-layered structures but have individual ferrioxamine-type intrastrand complexes. Fe_1-**3** exhibited a similar, slow constant iron-removal rate. This rate indicates that the iron resides at a single site and that Fe_1-**3** also has a ferrioxamine-type intrastrand structure. Complex Fe_3-**3**, in particular, possesses a clover-leaf type structure, as depicted in Scheme 2.

Protonation and EDTA exchange behavior of iron complexes

As the plots in Fig. 2 show, the three complexes of ligand **3** exhibited a high stability with wide plateaus, whereas narrower plateaus were observed for tripodal interstrand complexes Fe_1-**1**, Fe_1-**2** and Fe_2-**2**. These spans are much narrower than that (pH 3.7–10.5) determined for ferrichrome.[39] Fe_1-**1** has the lowest stability in this respect among the tripodal complexes.

The $K_{Fe(HL)}$ values also indicate that the complexes of **1** and **2** are more easily protonated than those of **3** and ferrichrome ($K_{Fe(HL)} = 31$);[40] Fe_1-**1** has the highest protonation tendency among all the present complexes. Fe_1-**3** and Fe_2-**3** show almost the same degree of monoprotonation stability, comparable with that of ferrioxamine D ($K_{Fe(HL)} = 3.2$),[40] reflecting a structural similarity. A slightly larger $K_{Fe(HL)}$ value for Fe_3-**3** is due to strain, which arises from the three intrastrand complexes being crowded together by the hydrophobic interactions of the ethylene and pentamethylene moieties.

When the rates of iron removal from Fe_1-**1**, Fe_1-**2** and Fe_2-**2** are compared, they are generally different except for those of Fe_1-**2** and of the lower site in Fe_2-**2**. The latter two cases indicate that the iron in Fe_1-**2** resides at the lower binding site and is removed at the same rate as that of Fe_2-**2**, since the same iron residence situation is left after the removal of the upper site iron in Fe_2-**2**.

It is reasonable to think that a repulsive force among the three terminal carboxylate anions acts as a destabilizing factor against the iron complex at the C-terminal site. Iron in ligand **2** prefers the lower site, because this site is remote from the terminal carboxylates and more stable for iron residence. This situation is revealed by a rate difference at pH 5.4 between Fe_1-**1** and Fe_1-**2**. The fact that the rate of removal from the upper site of Fe_2-**2** is slower than that of Fe_1-**1** can be attributed to a cooperative effect of the lower site iron binding to strengthen the iron binding at the upper site of Fe_2-**2**.

Notably, the rate constants observed for Fe_1-**3**, Fe_2-**3** and Fe_3-**3** were in the same range within about $\pm 10\%$, and these rates were close to the rate determined for a related complex, ferrioxamine B. But these small differences among the three complexes of **3** are real. As mentioned above, the iron complexes of **3** are all of the same intrastrand ferrioxamine type. Fe_2-**3** is considered as sterically hindered against attack by EDTA relative to Fe_1-**3**, and similarly Fe_3-**3** is much more hindered. This hindrance due to the crowdedness, as revealed in the larger monoprotonation value, makes Fe_3-**3** rather strained. When the strain is taken into account, this explains why its rate becomes slightly faster than that of Fe_2-**3**.

Thermodynamics of interstrand *vs.* intrastrand complexes

The tris(hydroxamato)iron(III) complexes of **1** and **2** were formed in a tripodal interstrand type, and those of **3** were formed in an intrastrand ferrioxamine type. For comparison of the thermodynamic stability between the two types, we chose two complexes, interstrand complex Fe_1-**2**, designated

as Fe(interstrand-L), and intrastrand complex Fe–{Ac–[Ahe–(O$^-$)Apr]$_3$–OMe}, designated as Fe(intrastrand-L). These complexes may not represent every aspect of their respective type, but they are considered as fair samples for comparing the two types.

The reaction of eqn. 5(a) is associated with the proton-dependent complex formation process and also allows us to assess the difference in the stability of the two complexes, when they are subjected to the iron-removal reaction separately. We assume that there is not much difference in the protonation constants of the hydroxamate groups between the two ligands. This assumption is reasonable, since a hydroxamate group in both ligands is located in the same unit sequence of a similar molecular environment.

We now show how the difference between the two complexes can be assessed. Each process of iron complex formation is expressed by eqns. 6(a) and 6(b), together with the free energy change:

$$H_3(\text{interstrand-L}) + Fe^{3+} = Fe(\text{interstrand-L}) + 3H^+ \quad \Delta G_1 \quad (6a)$$

$$H_3(\text{intrastrand-L}) + Fe^{3+} = Fe(\text{intrastrand-L}) + 3H^+ \quad \Delta G_2 \quad (6b)$$

Two equilibrium reactions performed for the examples of eqn. 5(a) are written as follows [eqns. 7(a) and 7(b)]:

$$Fe(\text{interstrand-L}) + H_2EDTA^{2-} + H^+ = Fe(EDTA)^- + H_3(\text{interstrand-L}) \quad (7a)$$

$$Fe(\text{intrastrand-L}) + H_2EDTA^{2-} + H^+ = Fe(EDTA)^- + H_3(\text{intrastrand-L}) \quad (7b)$$

for which $\Delta G^\circ = -41$ and -38 kJ mol^{-1}, respectively. By subtracting eqn. 7(b) from eqn. 7(a), we obtain eqn. 8,

$$Fe(\text{interstrand-L}) + H_3L(\text{intrastrand-L}) = Fe(\text{intrastrand-L}) + H_3(\text{interstrand-L}) \quad (8)$$

for which $\Delta G^\circ = -3$ kJ mol^{-1}. The same eqn. 8 can be derived by subtracting eqn. 6(a) from eqn. 6(b), that is, from the difference in the complex formation tendency of the intrastrand and interstrand type complexes ($\Delta G_2 - \Delta G_1$). The free energy, enthalpy and entropy changes of the reaction of eqn. 8 are calculated to be $\Delta G^\circ = -3$ kJ mol^{-1}, $\Delta H^\circ = -22$ kJ mol^{-1} and $\Delta S^\circ = -0.06$ kJ mol^{-1} K^{-1}. Thus, the temperature study of equilibrium iron-competition reactions with EDTA shows that the enthalpy change favors the formation of the ferrioxamine-type intrastrand complex.

Conclusions

Tripodal mono-, di- and tritopic hydroxamate ligands (**1**–**3**) of 1,3,5-benzene carboxylic acid derivatives carrying H–[Ahe–(HO)Apr]$_n$–OH ($n = 1, 2, 3$) strands linked by amide bonds have been synthesized. Each binding site of these ligands forms a tris(hydroxamato) complex with iron(III), producing Fe$_1$-**1**, Fe$_1$-**2**, Fe$_2$-**2**, Fe$_1$-**3**, Fe$_2$-**3** or Fe$_3$-**3**. Equilibrium protonation behavior indicated that all the complexes are of the intramolecular within-ligand type. Thus, the iron complexes of **1** and **2** have tripodal interstrand structures. A kinetic study of iron removal from individual complexes by excess EDTA characterized their structural features. Iron from complexes of **3** was removed more slowly than from **1** and **2**, and complexes Fe$_1$-**3**, Fe$_2$-**3** and Fe$_3$-**3** were assigned to each have individual ferrioxamine-type intrastrand structures; the structure of Fe$_3$-**3** thus has a clover-leaf pattern. The ferrioxamine-type intrastrand complexes existed over wider pH ranges and were protonated at lower pH than the interstrand complexes. Fe$_1$-**1** existed in a narrow pH region. One of the reasons for this was ascribed to electrostatic repulsion of the terminal carboxylate groups. Iron in the upper site of Fe$_2$-**2** was stable and kinetically inert relative to Fe$_1$-**1**, as a consequence of the cooperative binding effect by the lower site iron complexation. An equilibrium iron-exchange study indicated that the intrastrand complex is enthalpically more favored than the interstrand complex.

When tested, none of these iron complexes showed growth promotion activity for an *E. coli* mutant.

Experimental

General procedures

IR spectra were recorded on a JASCO model FT/IR-5M spectrophotometer. UV-vis spectra were obtained on a Hitachi 320A spectrophotometer. HPLC analysis was carried out on a JASCO 880-PU apparatus combined with 875-UV attachments, using a column (4.6 × 250 mm) of Finepac SIL C_{18}. A solvent system of CH_3CN–H_2O (3 : 1 v/v) containing 0.1% phosphoric acid was applied at a flow rate of 1 cm^3 min^{-1} and the retention time (R_t) was determined. ^{1}H NMR spectra were obtained in $CDCl_3$ or d^6-DMSO with JEOL FX-200, GX-270, EX-400 and A-500 spectrometers using tetramethylsilane as the internal standard. Purified ligands were used in the experiments. Mass spectra were recorded in the negative mode with a Micromass LCT mass spectrophotometer using the electrospray ionization (ESI) technique. The glass electrode in the pH meter was adjusted at three pH values (pH 4.01, 6.86 and 9.18) with standard buffer solutions as defined by the Japanese Industrial Standard (JIS Z 8802). The electrode system was calibrated to obtain a hydrogen-ion concentration from the pH-meter reading by titrating known amounts of HCl with CO_2-free NaOH solution in the low and high pH regions, and by determining the junction potentials.[41]

Syntheses

For complete details and characerization of the intermediate compounds, see electronic supplementary information.

General procedure for removal of the benzyl protective groups of 16–18 to produce 1–3. A tripodal protected ligand (one among **16**–**18**) was dissolved in MeOH and hydrogenated with H_2 in the presence of 10% Pd on carbon (100 wt%) for 36 h at room temperature and atmospheric pressure. The catalyst was separated and the solvent evaporated to give the crude product, which was purified by gel-chromatography with an HW-40 column (MeOH). Evaporating MeOH afforded the desired product.

C_6H_3[CO–Ahe–(HO)Apr–OH]$_3$ (ligand **1**) (0.0713 g, 93%) was obtained from **16** (0.102 g, 0.0948 mmol) as a white solid. HPLC: R_t 2.3 min. IR (KBr): $\nu_{C=O}$ 1722 (carboxylic acid), 1642 (amide) cm^{-1}. ^{1}H NMR (d^6-DMSO): δ 1.30–1.36 (m, 6H, 3 × NHCH$_2$CH$_2$C*H*$_2$CH$_2$CH$_2$CO), 1.48–1.58 (m, 12H, 3 × NHCH$_2$C*H*$_2$CH$_2$C*H*$_2$CH$_2$CO), 2.34 (t, $J = 7.5$, 6H, 3 × CH$_2$CO of Ahe), 2.41 (t, $J = 7.0$, 6H, 3 × CH$_2$CO of Apr), 3.28 (q, $J = 6.4$, 6H, 3 × NCH$_2$ of Ahe), 3.68 (t, $J = 6.8$, 6H, 3 × NCH$_2$ of Apr), 8.39 (s, 3H, C_6H_3), 8.69 (t, $J = 5.6$ Hz, 3H, 3 × C_6H_3–CON*H*). Anal. calc. for $C_{36}H_{54}N_6O_{15}\cdot H_2O$: C, 52.17; H, 6.81; N, 10.14%. Found: C, 52.24; H, 6.56; N, 9.84%.

C_6H_3[CO–Ahe–(HO)Apr–Ahe–(HO)Apr–OH]$_3$ (ligand **2**) (0.063 g, 74%) was obtained from **17** (0.118 g, 0.0605 mmol) as an amorphous solid. HPLC: R_t 2.1 min. IR (KBr): $\nu_{C=O}$ 1724 (carboxylic acid), 1639 (amide) cm^{-1}. ^{1}H NMR (d^6-DMSO): δ 1.22–1.57 [m, 36H, 6 × NHCH$_2$(C*H*$_2$)$_3$CH$_2$CO], 2.30–2.36 (m, 18H, 6 × CH$_2$CO of Ahe and 3 × CH$_2$CO of Apr), 2.40 (t, 6H, 3 × C*H*$_2$CO$_2$H), 3.01 (dt, $J = 5.5$ and 7.0, 6H, 3 × NCH$_2$ of Ahe), 3.28 (q, $J = 6.0$, 6H, 3 × NCH$_2$ of CO–Ahe), 3.67–

3.71 (m, 12H, 6 × NCH_2 of Apr), 7.85 (t, $J = 5.5$, 3H, 3 × NH), 8.37 (s, 3H, C_6H_3), 8.64 (t, $J = 5.5$ Hz, 3H, 3 × C_6H_3–CON*H*). Anal. calc. for $C_{63}H_{102}N_{12}O_{24} \cdot H_2O$: C, 52.93; H, 7.33; N, 11.76%. Found: C, 52.78; H, 7.54; N, 11.46%.

C_6H_3[CO–Ahe–(HO)Apr–Ahe–(HO)Apr–Ahe–(HO)Apr–OH]$_3$ (ligand **3**) (0.0316 g, 86%) was obtained from **18** (0.0515 g, 0.0183 mmol) as an amorphous solid. HPLC: R_t 2.8 min. IR (KBr): $\nu_{C=O}$ 1723 (carboxylic acid), 1635 (amide) cm^{-1}. ^1H NMR (d^6-DMSO): δ 1.23–1.53 [m, 54H, 9 × $NHCH_2(CH_2)_3CH_2CO$], 2.28–2.41 (m, 30H, 9 × CH_2CO of Ahe and 6 × CH_2CO of Apr), 2.41 (t, 6H, 3 × CH_2CO_2H), 2.99 (m, 12H, 6 × NCH_2 of Ahe), 3.16 (m, 6H, 3 × NCH_2 of CO–Ahe), 3.64–3.68 (m, 18H, 9 × NCH_2 of Apr), 7.89 (br t, 6H, 6 × NH), 8.36 (s, 3H, C_6H_3), 8.67 (br t, 3H, 3 × C_6H_3–CON*H*). Anal. calc. for $C_{90}H_{150}N_{18}O_{33} \cdot H_2O$: C, 53.24; H, 7.54; N, 12.41%. Found: C, 53.28; H, 7.49; N, 11.98%.

Iron(III) complex formation

A solution of ferric nitrate (3.60×10^{-3} M) in 0.1 M nitric acid was prepared by diluting a commercially available ferric nitrate standard solution with 0.1 M nitric acid. A ligand solution of 0.60 mM was prepared with doubly distilled deionized water. An aqueous stock solution of ligand **3** contained 15% DMF (v/v). Each iron(III) complex solution (2.0×10^{-4} M, a final volume of 3.0 mL, $I = 0.1$) was prepared by mixing the ligand solution (1.0 mL) and the ferric nitrate solution in water with KNO_3 (1.0 M; 0.3 mL) (pH meter reading, 2.2) and neutralizing to pH 7.0 with 0.1 or 1.0 M KOH. (In some cases precipitates appeared after mixing of the ligand and the acidic iron solution for a while, but disappeared as the complexation reaction proceeded). These complex-containing solutions were used for further study after 2-fold dilution (1.0×10^{-4} M, $I = 0.1$). The temperature was maintained at 25.0 ± 0.1 °C during measurements of UV-vis spectra.

Determinations of UV-vis spectral changes *vs.* pH were made by serial addition of HNO_3 (0.1 or 0.01 M) or KOH (0.1 or 0.01 M) to a neutral iron(III) complex solution and any changes in its volume due to the addition of acid or base were corrected. The presence of DMF (2.5%) had no practical effect on the pH-meter reading for every solution in the entire range (a shift of less than +0.02 pH unit).

Schwarzenbach plots were made using the spectral data that exhibited isosbestic points during gradual acidification. The presence of 2.5% DMF had no significant effect on the electrode calibration. However, the accuracy of $K_{Fe(HL)}$ values less than 30 should be considered with care because of the limitations of electrode function.

Mass spectrometry of iron complexes

The formation of intramolecular iron(III) complexes was further confirmed by the ESI mass spectra using samples prepared by mixing the ligand and ferric hydroxide made *in situ* in water; Fe_2-**2** (H_2O–MeCN, 1 : 1 v/v): *m/z* 757.3 $[M - 2H^+]^{2-}$; Fe_3-**3** (H_2O–MeCN, 1 : 1 v/v): *m/z* 1084.4 $[M - 2H^+]^{2-}$ and 722.6 $[M - 3H^+]^{3-}$.

Iron(III) exchange with EDTA

Rate determinations. Each of these exchange reactions was performed at 25 °C in a 10-mm cell containing a solution of 2.5 mL of a pH 5.4 AcOH–AcONa buffer (40 mM) maintained at ionic strength 0.1 with KNO_3. The iron(III) complex concentration was 1.0×10^{-4} M, and the reaction was initiated by adding a 50 μL EDTA solution (0.1 M); final EDTA concentration was 2.0×10^{-3} M. The reaction was monitored by following the decrease in absorbance at 420 nm and it was found to obey a first-order rate law. The pseudo-first-order rate constant was determined from the slope of the plot of $\ln[(A_t - A_\infty)/(A_0 - A_\infty)]$ *vs.* time, where A_0, A_∞ and A_t denote, respectively, absorbances at the initial time, at the final time and at time *t*, and the first-order rate law was followed in most cases for 4 half-lives. The rate was obtained with an error of ±5% by averaging at least two determinations. In the case of the consecutive reactions for Fe_2-**2**, two pseudo-first-order rate constants (k_1^{up} and k_1^{low}) were obtained by curve fitting the data (40 data points) to eqn. 4 within the indicated error limit. DMF (2.5%) in the solution had no effect on the rates.

Equilibrium determinations. Each of the equimolar reactions was carried out under the conditions shown in Table 3, by following the decrease in the absorbance of Fe(L) at 420 nm periodically, without the use of any buffer. As the reaction progressed toward equilibrium, the pH of the solution changed and was adjusted periodically, to 5.4 with 0.1 M KOH solution. More than 3 weeks was needed for the equilibration. A value of $\varepsilon = 52$ M^{-1} cm^{-1} (420 nm) was used for correcting the spectral intensity for the presence of $Fe(EDTA)^-$.

Biological assay

Growth promotion tests were performed by the standard paper-disc procedure using a mutant, *E. coli* K-12 RW 193 (ATCC 33475).[12] The bacto nutrient agar medium (10 mL) contained 2.0 mM ethylenediamine di(*o*-hydroxyphenylacetic acid) and two drops of the test strain. Filter paper discs (6 mm diameter) were impregnated with 10 μL of each ligand (1.0 mM) or their iron complex (0.1 mM) solution (50% DMF in water) and placed on the plate. Water was used as a blank. The diameter of the growth response zone was checked against a reference provided with desferrichrome (0.5 mM) and desferrioxamine B after 48 h at 37 °C. With the former and the latter as references, growth promotion diameter zones of 20 and 16 mm were observed, but no growth zone was detected with the ligands and their iron(III) complexes.

Acknowledgements

We thank JASCO International Co., Ltd. for recording the ESI mass spectra of the iron(III) complexes.

References

1 *Iron Transport in Microbes, Plants and Animals*, ed. G. Winkelmann, D. van der Helm and J. B. Neilands, VCH Publishers, Weinheim, 1987.
2 J. B. Neilands, *J. Biol. Chem.*, 1995, **45**, 26723.
3 *Handbook of Microbial Iron Chelates*, ed. G. Winkelmann, CRC Press, Boca Raton, FL, 1991.
4 B. F. Matzanke, G. Müller-Matzanke and K. N. Raymond, in *Iron Carriers and Iron Proteins*, ed. T. M. Loehr, Physical Bioinorganic Chemistry Series, vol. 5, VCH Publishers, New York, 1989, p. 3.
5 B. F. Matzanke, in *Encyclopedia of Inorganic Chemistry*, ed. R. B. King, John Wiley & Sons, Chichester, 1994, vol. 4, p. 1915.
6 R. C. Hider, *Struct. Bonding*, 1984, **58**, 25.
7 T. Emery, in *Metal Ions in Biological Systems*, ed. H. Sigel, Marcel Dekker, New York, 1978, vol. 7, ch. 3, p. 77.
8 W. Keller–Schierlein, V. Prelog and H. Zähner, *Fortschr. Chem. Org. Naturst.*, 1964, **22**, 279.
9 D. van der Helm, M. A. F. Jalal and M. B. Hossain, in *Iron Transport in Microbes, Plants and Animals*, ed. G. Winkelmann, D. van der Helm and J. B. Neilands, VCH Publishers, Weinheim, 1987, p. 135.
10 A. Zalkin, J. D. Forrester and D. H. Templeton, *J. Am. Chem. Soc.*, 1966, **88**, 1810.
11 D. van der Helm and M. Poling, *J. Am. Chem. Soc.*, 1976, **98**, 82.
12 J. B. Neilands, *Struct. Bonding*, 1984, **58**, 1.
13 G. Müller and K. N. Raymond, *J. Bacteriol.*, 1984, **160**, 304.
14 V. Braun and G. Winkelmann, *Prog. Clin. Biochem. Med.*, 1987, **5**, 67.
15 S. A. Leong and G. Winkelmann, in *Metal Ions in Biological Systems*, ed. A. Sigel and H. Sigel, Marcel Dekker, New York, 1998, vol. 35, p. 147.

16 M. L. Guerinot, *Annu. Rev. Microbiol.*, 1994, **48**, 743.
17 A. L. Crumbliss, in *Handbook of Microbial Iron Chelates*, ed. G. Winkelmann, CRC Press, Boca Raton, FL, 1991, ch. 7, p. 177.
18 A.-M. Albrecht–Gary and A. L. Crumbliss, in *Metal Ions in Biological Systems*, ed. A. Sigel and H. Sigel, Marcel Dekker, New York, 1998, vol. 35, p. 239.
19 A. Shanzer and J. Libman, in *Handbook of Microbial Iron Chelates*, ed. G. Winkelmann, CRC Press, Boca Raton, FL, 1991, p. 309.
20 I. Yoshida, I. Murase, R. J. Motekaitis and A. E. Martell, *Can. J. Chem.*, 1983, **61**, 2740.
21 A. E. Martell, R. J. Motekaitis, I. Murase, L. F. Sala, R. Stoldt, C. Y. Ng, H. Rosenkrantz and J. J. Metterville, *Inorg. Chim. Acta*, 1987, **138**, 215.
22 B. H. Lee, M. J. Miller, C. A. Prody and J. B. Neilands, *J. Med. Chem.*, 1985, **28**, 317.
23 M. S. Mitchell, D.-L. Walker, J. Whelan and B. Bosnich, *Inorg. Chem.*, 1987, **26**, 396.
24 M. Akiyama, A. Katoh and T. Ogawa, *J. Chem. Soc., Perkin Trans. 2*, 1989, 1213.
25 K. Shimizu and M. Akiyama, *J. Chem. Soc., Chem. Commun.*, 1985, 183.
26 H. Dugas, *Bioorganic Chemistry*, Springer–Verlag, New York, 3rd edn., 1998, ch. 8, p. 593.
27 S. Blanc, P. Yakirevitch, E. Leize, M. Meyer, J. Libman, A.V. Dorsselaer, A. Albrecht–Gary and A. Shanzer, *J. Am. Chem. Soc.*, 1997, **119**, 4934.
28 *Development of Iron Chelators for Clinical Use*, ed. A. E. Martell, W. F. Anderson and D. G. Badman, Elsevier/North Holland, New York, NY, 1981.
29 *The Development of Iron Chelators for Clinical Use*, ed. R. J. Bergeron and G. M. Brittenham, CRC Press, Boca Raton, FL, 1994.
30 K. Shimizu, K. Nakayama and M. Akiyama, *Bull. Chem. Soc. Jpn.*, 1984, **57**, 2456.
31 W. König and R. Geiger, *Chem. Ber.*, 1970, **103**, 788.
32 Y. Hara and M. Akiyama, *Inorg. Chem.*, 1996, **35**, 5173.
33 G. Schwarzenbach and K. Schwarzenbach, *Helv. Chim. Acta*, 1963, **46**, 1390.
34 M. T. Caudle, R. D. Stevens and A. L. Crumbliss, *Inorg. Chem.*, 1994, **33**, 843 and 6111.
35 T. P. Tufano and K. N. Raymond, *J. Am. Chem. Soc.*, 1981, **103**, 6617.
36 A.-M. Albrech–Gary, T. Palanche–Passeron, N. Rochel, C. Hennard and A. M. Abdallah, *New J. Chem.*, 1995, **19**, 105.
37 Y. Hara, L. Shen, A. Tsubouchi, M. Akiyama and K. Umemoto, *Inorg. Chem.*, 2000, **39**, 5074.
38 R. G. Wilkins, *Kinetics and Mechanisms of Reactions of Transition Metal Complexes*, 2nd edn., VCH, Weinheim, 1991, ch. 1.
39 M. Akiyama, A. Katoh and T. Mutoh, *J. Org. Chem.*, 1988, **53**, 6089.
40 G. Anderegg, F. L'Eplattenier and G. Schwarzenbach, *Helv. Chim. Acta*, 1963, **46**, 1400 and 1409.
41 H. M. Irving, M. G. Miles and L. D. Pettit, *Anal. Chim. Acta*, 1967, **38**, 475.